

Synthesis, Characterization, Antibacterial and Anticancer Properties of Silver Nanoparticles Synthesized from Carica Papaya Peel Extract

Tessy John^{1,*}, Kokila A. Parmar², Shailesh C. Kotval² and Jayesh Jadhav²

¹Department Physics, Faculty of Science, Pacific University, Udaipur, Rajasthan, India

²Department Chemistry, Faculty of Science, HNG University, Patan, Gujarat, India

(*) Corresponding author: tessyjohn45@gmail.com

(Received: 07 May 2018 and Accepted: 13 August 2018)

Abstract

In the present generation, there is a commercial demand for silver nanoparticles due to their widespread applications. In this study, silver nanoparticles were synthesized using Carica papaya peel extract as a reducing agent. The synthesized nanoparticles were characterized under UV-Visible spectrophotometer, FTIR, SEM, XRD and TEM. UV-Visible spectrophotometer was used to monitor the formation of silver nanoparticles. The TEM analysis shows that the silver nanoparticles have an average size of 50 nm. X-ray diffraction analysis showed that the particles were crystalline in nature. The antibacterial activity of silver nanoparticles was performed on various gram-positive and gram-negative bacteria. These silver nanoparticles showed a significant cytotoxic effect against both, MCF-7 and Hep-2 cells.

Keywords: Green synthesis, Antimicrobial activity, Anticancer activity, Silver nanoparticles.

1. INTRODUCTION

Noble metal nanoparticles have found widespread use in several applications such as optics, biomedical sciences, drug delivery, catalysis and electronics [1-3]. The unique property of nanoparticles is that they exhibit larger surface area to volume ratio [4-9]. Metal nanoparticles such as gold, silver, copper and platinum can be synthesized by physical, chemical and biological methods. The physical methods include laser ablation method, arc discharged method, high energy ball-milling method and the chemical vapor deposition. The chemical method includes co-precipitation method, sol-gel method, micro-emulsion method, hydrothermal method, sono-chemical method and microwave method [10-13]. Since synthesis of nanoparticles by physical and chemical methods may have considerable environmental defect, biogenic synthesis of metal nanoparticles has become a major

focus for researchers. The synthesis of nanoparticles using various plants and their extracts can be advantageous over other biological synthesis, as the plants are widely distributed, easily available, much safer to handle and act as a source of several metabolites [14-22].

In the present generation, there is a commercial demand or silver nanoparticles due to their widespread applications. It has been already proved that different parts of plant materials such as fruit, bark, fruit peels, root and callus have been used for the synthesis of silver nanoparticles in different sizes and shapes. A recent study revealed that silver nanoparticles synthesized using *Azadirachta indica* leaf extract displayed potential antimicrobial activity against water-borne pathogens [23]. There have also been several experiments performed on the synthesis of silver nanoparticles using *Asparagus racemosus*,

[24] Bauhinia variegata, [25] Moringa oleifera [26] and Ocimum sanctum [27] in the field of biomedicine.

2. MATERIALS AND METHODS

2.1. Synthesis of Silver Nanoparticles

Silver nitrate was purchased from Sigma Aldrich chemicals. Glassware was cleaned and washed with double distilled water to remove any impurities and dried in an oven before use. Fresh Papaya peels were collected and rinsed thoroughly with distilled water and dried at room temperature. The peels were finely powdered and used for preparation of the extract. The plant sample was weighed and soaked with 250ml of methanol at room temperature for two days. The extract was filtered through whatman no.1 filter paper. 0.1M AgNO₃ was prepared by dissolving 4.25g AgNO₃ in 250ml double distilled water. The reaction mixture was prepared by adding 100ml of the plant extracts to 100ml of 0.1M AgNO₃ solution in a 250 ml round bottom flask. The mixture was stirred for 2 h at room temperature; slowly the color started changing from colorless to brown and finally reddish brown. It showed that aqueous silver ions could be reduced by the methanol extract of papaya peel to generate silver nanoparticles.

3. CHARACTERIZATION OF SILVER NANOPARTICLES

3.1. UV-Vis Studies of Silver Nanoparticles

The reduction of silver nitrate to pure Ag⁺ ions using methanol extract of papaya peel was recorded using a UV-Vis spectrophotometer. The sample was diluted with 3 ml of acetone and measured for UV-Vis spectrum at room temperature in the range of 200–800 nm. Acetone was used as a reference.

3.2. FTIR Analysis

FTIR measurement was carried out for both extract and Silver nanoparticles to identify the biomolecules present in the extract of papaya peel and biomolecules

within the Silver nanoparticles. FTIR spectra of the methanol extract of papaya peel and the purified silver nanoparticles powder were analyzed by FTIR spectroscopy. FTIR spectra were measured using the KBr pellet technique with spectrometer in the 4000-400 cm⁻¹ range of wave number. The bio-reduced solution was centrifuged at 2500rpm for 30 minutes at room temperature and the pellet was obtained. The pellet was re-dispersed in distilled water. The process of centrifugation and re-dispersion in sterile water was repeated thrice. Then, the purified silver nanoparticles were dried in the oven at 100°C. The FTIR spectrum of the dried sample was carried out to study the possible functional groups responsible for the formation of silver nanoparticles.

3.3. SEM, TEM Analysis of Silver Nanoparticles

The Scanning Electron Microscope (SEM) has been employed for the morphological characterization of the synthesized silver nanoparticles. Morphological evaluation of the silver nanoparticles was carried out using Scanning electron microscope with an accelerated voltage of 20 KV. The size and shape of the resultant particles was visualized with the help of Transmission Electron Microscopy [TEM].

3.4. X-ray Diffraction (XRD Analysis)

The purified silver nanoparticles characterized by XRD to determine the crystal structure of the produced nanoparticles. The average crystalline size of the synthesized silver nanoparticles was calculated using Scherrer's formula

$$D = \frac{0.9\lambda}{\beta \cos\theta}$$

D = Average crystalline size

λ = X – Ray wavelength

β = FWHM

θ = Diffraction angle

XRD pattern was recorded using an XRD – 6000 X-ray diffractometer (Shimadzu Kyoto-Japan) operated at a voltage of 40 KV and 30 Ma with Cu α radiation in $\theta - 2\theta$ configurations.

4. ANTIBACTERIAL ACTIVITY OF SILVER NANOPARTICLES

The antibacterial activity performed by antimicrobial susceptibility tests, NCCLS 1993, Approved standard: M2-A5. *E. Coli* (Gram negative), *S.aerious* (Gram positive), *K. pneumonia* (Gram negative), *P.aeruginosa* (Gram negative) strains were used for the antibacterial activity.

The minimum inhibitory concentration (MIC) of compounds for each test organism was determined by a modification of the broth dilution method performed in 96 well micro-trays (NCCLS, 1993). A stock solution of extract was made in dimethyl sulphoxide (DMSO). Three-fold serial dilutions of the reconstituted compounds (150 μ l) of each sample were made in sterile broth (nutrient broth) to achieve a concentration range of 1.95-1000 μ g/ml. The amount of test organisms (50 μ l) was added to each dilution to give a final volume of 200 μ l. After incubation at 37°C for 18–24hrs, the plates were examined for growth of the organisms. The lowest concentration that inhibited growth was recorded as the MIC. Growth was determined as the difference in absorbance at 595nm between reading taken before and after incubation of the plates. Readings less than 20% of the positive control were recorded as inhibition. Absorbance was read in a plate reader. Four replicates were performed for extract against each of the test organisms. Positive (50 μ l cells + 150 μ l medium) and negative (200 μ l medium). Controls were performed with each experiment. Each plate also included a solvent control in which 100 μ l of the appropriate diluted solvent was added to 100 μ l of the test organism. The data analysis was accomplished using Graph Pad InStat version 3.00 for Windows 95, GraphPad

Software Inc., San Diego California USA. IC50 values were obtained from regression lines with coefficient factors between $R^2 = 0.52$ and 0.99 . Absorbance at 595nm between reading taken before and after incubation of the plates.

5. IN-VITRO CYTOTOXICITY ANALYSIS

The nano-metallic compounds were studied against various cell line named MCF-7 and HEP-2 along with standard anticancer drug i.e. Methotrexate. MCF-7 and HEP-2 cell cultures were used in these experiments were derived from National Centre for Cell Science (NCCS), Pune. Stock cells of these cell line was cultured in DMEM, supplemented with 10% FBS (fetal bovine serum). Along with media cells were also supplemented with 5 % HBSS, penicillin, streptomycin and Amphotericin-B, in a humidified atmosphere of 5% CO₂ at 37°C until confluence reached. The cells were dissociated with 0.2% trypsin, 0.02% EDTA in phosphate buffer saline solution. The stock cultures were grown initially in 25cm² tissue culture flasks, then in 75cm² and finally in 150cm² tissue culture flask and all cytotoxicity experiments were carried out in 96 microtiter well-plates. 2 \times 10⁴ cells/well was added in to each well of 96 well-plates. Cell lines in exponential growth phase were washed, trypsinized and re-suspended in complete culture media. Cells were seeded at 2 \times 10⁴ cells / well in 96 well microtiter plate and incubated for 24 hrs, during which a partial monolayer was formed. The cells were then exposed to various concentrations of the test compounds (as indicated in plate assignment) and standard doxorubicin. Control wells were received only maintenance medium. The plates were incubated at 37°C in a humidified incubator with 5% CO₂, 75% Relative Humidity for a period of 24 hrs. Morphological changes of drug treated cells were examined using an inverted microscope at different time intervals and

compared with the cells serving as control. At the end of 24 hrs, cellular viability was determined using MTT assay. Absorbance values that are lower than the control cells indicate a reduction in the rate of cell proliferation. Conversely, a higher absorbance rate indicates an increase in cell proliferation. Rarely, an increase in proliferation may be offset by cell death; evidence of cell death may be inferred from morphological changes. After 24 hrs, the cytotoxicity data was evaluated by determining absorbance and calculating the correspondent chemical concentrations. Linear regression analysis with 95 % confidence limit and R^2 were used to define dose-response curves and to compute the concentration of chemical agents needed to reduce absorbance of the formazan by 50% (IC_{50}). Dose Response Curve (DRC) against all cell lines was plotted with 10 analysis point i.e. with 10 different drug concentrations. The concentration causing 50% cell growth inhibition (IC_{50}) was determined from DRC using *Graph Pad Prism* software (Ver. 5.04) (Graph Pad Software, Inc., USA) and Microsoft Excel 2007 (Microsoft Corporation, USA) application.

6. RESULT AND DISCUSSION

6.1. UV- Visible Spectrophotometer Analysis

Silver nanoparticles were synthesized rapidly within 15 minutes of incubation period. The aqueous silver nitrate solution was turned to reddish brown color with the addition of papaya peel extract. Color change may be due to the excitation of surface Plasmon resonance effect and reduction of $AgNO_3$. The synthesis of silver nanoparticles by using methanol extract of papaya peel easily monitored by using UV-Visible spectrophotometer and the peak absorbance was noticed at around 400 nm. Figure 1 shows the UV-vis absorption spectrum of the synthesized Ag nanoparticles.

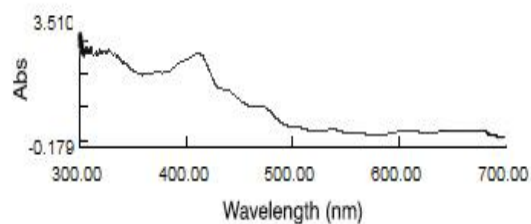


Figure 1. UV-Visible spectra analysis of silver nanoparticles.

6.2. Fourier Transform Infrared Spectroscopy (FTIR)

FTIR measurements of both the papaya peel extract and the synthesized silver nanoparticles were carried out to identify the possible biomolecules for capping and efficient stabilization of the nanoparticles. The FTIR spectra of the silver nanoparticles are shown in figure 2. The spectrum showed several peaks at 3317.56, 2852.72, 1660.71, 1463.97, 719.45, 626.87, 584, 43, and 538.14 cm^{-1} . The peak value at 3317.56 cm^{-1} corresponds to O-H stretching of H-bonded alcohols and phenols. The peak value at 2852.72 cm^{-1} corresponds to O-H stretching of carboxylic acids. The peak value at 1660.71 cm^{-1} corresponds to N-H bending of primary amines. The peak value at 1463.97 cm^{-1} corresponds to C-C stretching of aromatic ring structure. The peak values at 626.87 cm^{-1} and 719.45 cm^{-1} corresponds to C-H stretching of aromatic compounds. The peaks at 538.14 cm^{-1} and 584.43 cm^{-1} indicates OH bending of the phenolic group. From the FTIR spectrum it was confirmed that reduction and stabilization of silver nanoparticles is due to phytoconstituents that present in the papaya peel extract. It has the ability to perform dual functions of reduction and stabilization of silver nanoparticles.

6.3. SEM and TEM Analysis of Silver Nanoparticles

The SEM micrograph shows the surface morphology of silver nanoparticles. It was shown that relatively uniform and spherical shaped silver nanoparticles were formed.

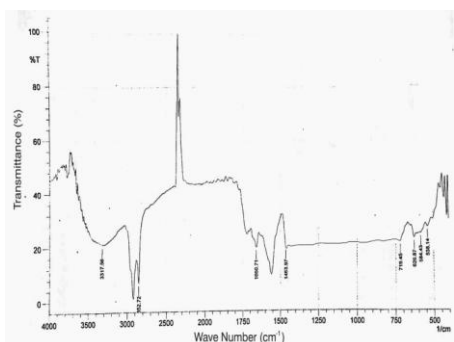


Figure 2. FTIR spectra of silver nanoparticles.

Similar results were obtained where the SEM micrograph shows crystalline spherical silver nanoparticles [28]. The size and shape of the silver nanoparticles were analyzed by TEM. TEM images showed that silver nanoparticles are spherical in shape with an average size of 50 nm.

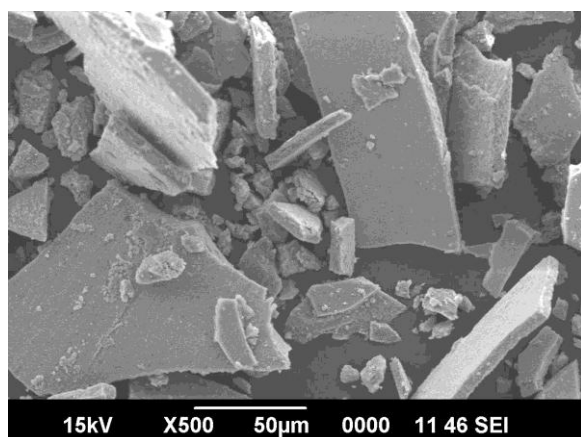


Figure 3. Scanning electron microscopic image of silver nanoparticles.

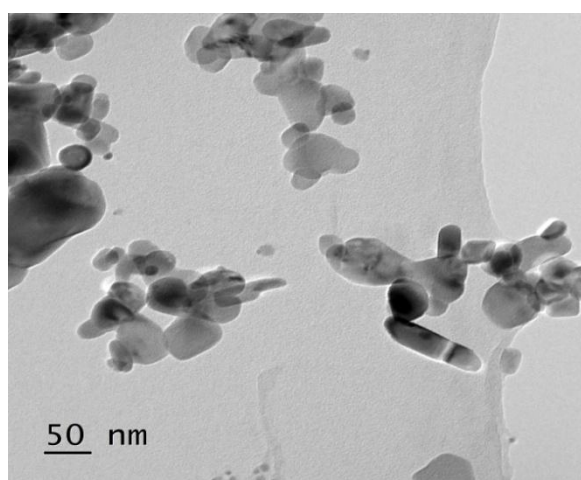


Figure 4. TEM image of silver nanoparticles.

6.4. X-ray Diffraction Analysis (XRD)

The crystalline nature of Silver nanoparticles was determined by the analysis of XRD pattern as shown in figure. The diffraction spectrum of the biologically synthesized nanoparticles showed distinct diffraction peaks at 27.82° , 32.3° , 38.25° , 46.25° , 54.79° , 57.33° and 77.03° can be indexed to the (1 1 1), (2 0 0), (2 1 1), (2 2 0), (3 1 1), (2 2 2), and (4 2 0) planes of face centered cubic structure of Silver. In addition to the Bragg peaks, additional peak were also observed at 64.45° . This is due to the organic compounds which are present in the extract and responsible for silver ions reduction and stabilization of resultant nanoparticles. The average particle size of the silver nanoparticle is 12.84 nm as calculated by Debye – Scherrer formula.

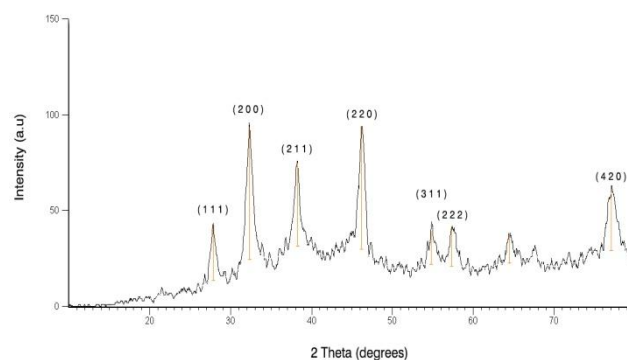


Figure 5. XRD spectrum of silver nanoparticles.

6.5. Anti-bacterial Activity of Silver Nanoparticles

Antibacterial activity of silver nanoparticle was evaluated against the following micro-organisms: *Escherichia coli*, *Klebsiella pneumonia*, *Pseudomonas aeruginosa* (Gram negative) *Staphylococcus aureus* (Gram positive). Silver nanoparticles showed antibacterial activity against almost all the test organisms. The mechanism involved in antibacterial activity of silver nanoparticle is that it may attach to the surface of the cell membrane disturbing permeability,

osmoregulation, electron transport and respiration.

The figures showed the plot of log concentration Vs % cell inhibition of test compound against tested organisms. Test extract show the dose-effect co-relation with maximum linearity in almost all cases within 0.84 to 0.99. The antibacterial activity of silver nanoparticles was size dependent. From above results we can conclude that test papaya peel extract showed maximum antibacterial activity against gram negative bacteria and least activity against gram positive. Similar results were obtained by Velusamy et al. (2015). This could be due to the presence of thicker peptidoglycan layer in gram positive than gram negative bacteria preventing the entry of silver nanoparticles and its antibacterial activity [29]. The antibacterial activity is certainly due to the silver cations released from silver nanoparticles that acts as reservoirs for the Ag⁺ bactericidal agent. Big changes in the membrane structure of bacteria as a result of the interaction with silver cations lead to the increased membrane permeability of the bacteria. Gram positive bacteria are composed of a three-dimensional thick peptidoglycan layer compared to that of gram negative bacteria [30]. The peptidoglycan layer possessing linear polysaccharide chain is cross linked by more short peptides thus forming a complex structure leading to difficult penetration of silver nanoparticles into gram positive bacteria compared to that of gram negative bacteria.

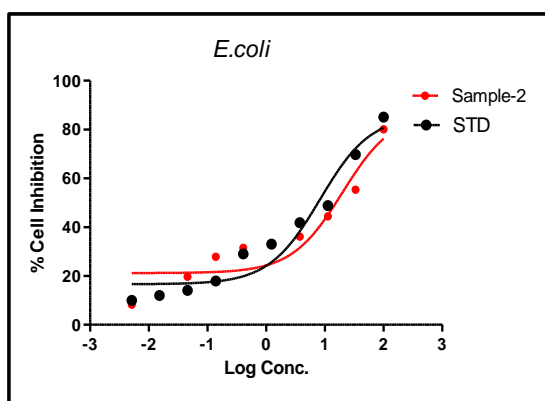


Figure 6. Plot of log concentration Vs % cell inhibition of test compound against *Escherichia coli* strain.

Table 1. Percentage cell inhibition by test compounds against *Escherichia coli* strain.

Conc (µM/ml)	Log Conc.	% Cell inhibition	
		Sample	STD
0.01	-2.29	8.23	9.97
0.02	-1.82	11.68	11.96
0.05	-1.34	19.65	14.06
0.14	-0.86	27.82	17.94
0.41	-0.39	31.52	29.02
1.23	0.09	33.26	33.01
3.70	0.57	36.12	41.85
11.11	1.05	44.37	48.87
33.33	1.52	55.37	69.72
100.00	2.00	80.11	85.06
IC50 µl/ml		19.90	8.198
R²		0.8695	0.9467

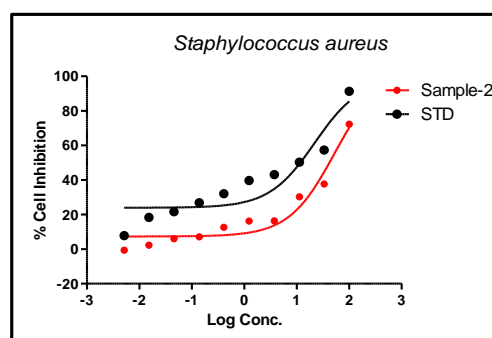


Figure 7. Plot of log concentration Vs % cell inhibition of test compound against *Staphylococcus aureus* strain.

Table 2. Percentage cell inhibition by compounds against *Staphylococcus aureus* strain.

Conc (µM/ml)	Log Conc.	% Cell inhibition	
		Sample	STD
0.01	-2.29	-0.58	7.86
0.02	-1.82	2.35	18.34
0.05	-1.34	6.021	21.63
0.14	-0.86	7.125	26.87

0.41	-0.39	12.68	32.08
1.23	0.09	16.23	39.67
3.70	0.57	16.37	43.08
11.11	1.05	30.27	50.34
33.33	1.52	37.65	57.34
100.00	2.00	72.30	91.34
IC50 μl/ml		51.94	21.88
R²		0.942	0.8576

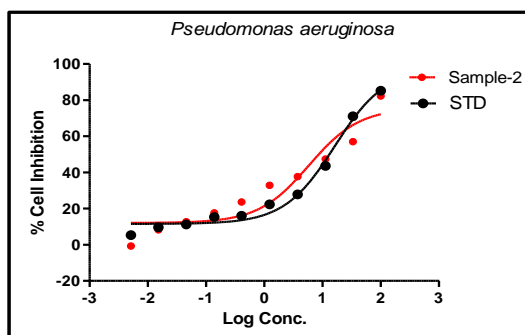


Figure 8. Plot of log concentration Vs % cell inhibition of test compound against *Pseudomonas aeruginosa* strain.

Table 3. Percentage cell inhibition by compounds against *Pseudomonas aeruginosa* strain.

Conc (μ M/ml)	Log Conc	% Cell inhibition	
		Sample	STD
0.01	-2.29	-0.652	5.32
0.02	-1.82	8.235	9.652
0.05	-1.34	12.752	11.25
0.14	-0.86	17.682	15.34
0.41	-0.39	23.652	16.05
1.23	0.09	32.872	22.31
3.70	0.57	37.682	27.88
11.11	1.05	47.382	43.62
33.33	1.52	57.032	71.05
100.00	2.00	82.342	85.26
IC50 μl/ml		5.805	16.19
R²		0.8990	0.9862

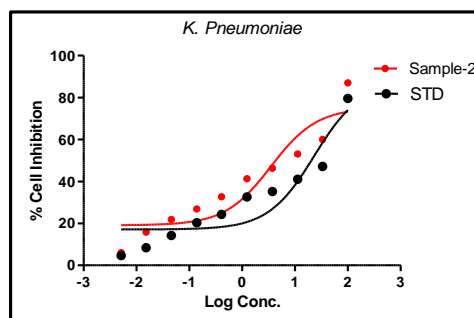


Figure 9. Plot of log concentration Vs % cell inhibition of test compound against *Klebsiella pneumoniae* strain.

Table 4. Percentage cell inhibition by compounds against *Klebsiella pneumoniae* strain.

Conc (μ l/ml)	Log Conc	% Cell inhibition	
		Sample	STD
0.01	-2.29	6.032	4.652
0.02	-1.82	15.863	8.362
0.05	-1.34	21.852	14.230
0.14	-0.86	26.872	20.320
0.41	-0.39	32.687	24.310
1.23	0.09	41.321	32.650
3.70	0.57	46.302	35.240
11.11	1.05	53.128	41.050
33.33	1.52	60.021	47.120
100.00	2.00	87.021	79.550
IC50 μl/ml		3.489	22.95
R²		0.8625	0.8497

From the above results, we can conclude that test papaya peel extract showed maximum antibacterial activity against *Pseudomonas aeruginosa* (Gram negative bacteria) and least activity against *S.aeriosus*(Gram positive).

6.6. In-vitro cytotoxicity Analysis

The in-vitro cytotoxicity effect of silver nanoparticles was studied against Hep-2 cell and MCF-7 cell line at different concentration 0.05, 0.15, 0.46, 1.37.4.12, 12.35, 37.04, 111.11, 333.33, and 1000. The concentration required for 50% cell death (IC50) for MCF-7 and HEP-2 cell line were found to be 35.19 and 83.06 respectively. IC50 value was found to be less for the MCF -7 cell line than HEP -2 cell line.

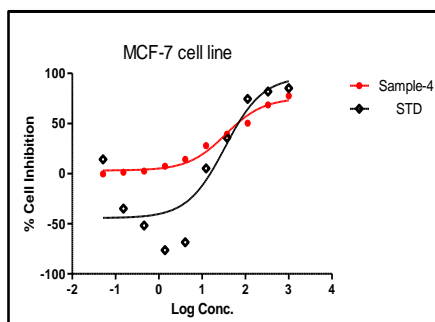


Figure 10. Anticancer effect of silver nanoparticles on MCF-7 cell lines.

Table 5. % Cell inhibition of MCF-7 cells by tests compounds at different concentration.

Concentration	Log Concentration	% Cell Inhibition	
		Sample	STD
0.05	-1.29	-0.3241	14.2400
0.15	-0.82	1.3524	-34.9400
0.46	-0.34	2.5682	-51.7500
1.37	0.14	7.3254	-76.3400
4.12	0.61	14.2351	-68.5000
12.35	1.09	27.8532	5.1200
37.04	1.57	39.2142	35.7800
111.11	2.05	50.3241	74.4500
333.33	2.52	68.5621	81.8652
1000	3.00	77.5471	85.2631
IC₅₀ (µg/ml)		35.19	33.58
R²		0.9795	0.8040

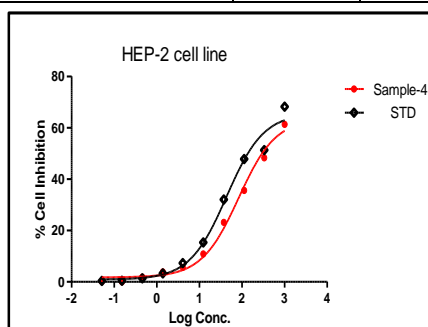


Figure 11. Anticancer effect of silver nanoparticles on Hep-2 cell line

Table 6. % Cell inhibition of HEP-2 cells by tests compounds at different concentration.

Concentration	Log Concentration	% Cell Inhibition	
		Sample	STD
0.05	-1.29	0.154	0.352
0.15	-0.82	0.029	0.412
0.46	-0.34	1.852	1.365
1.37	0.14	3.874	3.287
4.12	0.61	5.652	7.298
12.35	1.09	10.85	15.34
37.04	1.57	23.16	32.01
111.11	2.05	35.62	47.85
333.33	2.52	48.26	51.32
1000	3.00	61.32	68.21
IC₅₀ (µg/ml)		83.06	43.47
R²		0.992	0.986

7. CONCLUSION

Green chemistry nanoparticles are gaining importance as it is cost-effective, safe, non-toxic, and is eco-friendly. The biological process for the formation of silver nanoparticles using methanolic extract of carica papaya peel has been demonstrated. The synthesized silver nanoparticles were characterized using UV-Visible spectrophotometer, FTIR, SEM, XRD and TEM. The FTIR spectrum indicated the functional groups present as capping agent in the formation of silver nanoparticles. TEM analysis showed that the average size of synthesized silver nanoparticles is around 50 nm. The XRD studies reveal that silver nanoparticles are crystalline in nature with an average size of 12.84 nm. The obtained silver

nanoparticles showed significant anti-bacterial and anticancer activity.

ACKNOWLEDGEMENT

The authors are sincerely thankful to the following institutions: Sanjivani College of

Pharmaceutical Education and Research (Shinganapur, Ahmednagar, India) and Sophisticated Instrumentation Centre, Kochi University (Kochi, India), for providing laboratory facilities and Instrumentation.

REFERENCES

1. Laura, Ch., Singaravelu, V., Manjusri M., Amar Kumar M., "Biosynthesis of silver nanoparticles using murrayakoenigii (curry leaf): An investigation on the effect of broth concentration in reduction mechanism and particle size", *Adv. Mat. Lett*, 6 (2011) 429-434.
2. Karimzadeh R., Mansour N., "Effect of concentration on the thermo-optical properties of colloidal silver nanoparticles", *J. Pptlastec*, 5 (2010) 783-789.
3. Sun, R. W., Chen, R., Chung, N. P., Ho, C M., Lin, C. L., Che, C. M., "Silver nanoparticles fabricated in Hepes buffer exhibit cytoprotective activities toward HIV-1 infected cells", *Chem commun (Camb)*, 28 (2005) 5059-5061.
4. Ramesh Kumar, P., Singaravelu, V., Manjusri M., Amar Kumar M., Nallani S., "Soybean (Glycine max) leaf extract based green synthesis of palladium nanoparticles", *JBNB*, 3 (2012) 14-19.
5. Cheong, S., Watt, J. D., Tilley, R. D., "Shape control of platinum and palladium nanoparticles for catalysis", *Nanoscale*, 10 (2010) 2045-2053.
6. Jha, A. K., Prasad, K., Kulkarni, A. R., "Yeast mediated synthesis of silver nanoparticles", *International Journal of Nanoscience and Nanotechnology*, 4 (2008) 17-22.
7. Chen, H., Wei, G., Ispas, A., Hickey, S. G., Iler, A. E., "Synthesis of palladium nanoparticles and their applications for surface-enhanced raman scattering and electrocatalysis", *The Journal of Physical Chemistry C*, 50 (2010) 21976-21981.
8. Vala, A. K., Shah, S., "Rapid synthesis of silver nanoparticles by a marine-derived fungus *Aspergillus Niger* and their antimicrobial potentials", *International journal of nanoscience and nanotechnology*, 8 (2012) 197-206.
9. Gopidas, K. R., Whitesell, J. K., Fox, M. A., "Synthesis, characterization, and catalytic applications of a Palladium-nanoparticle-cored dendrimer", *Nano Letters*, 12 (2003) 1757-1760.
10. Honary, S., Gharaei-Fathabad, E., Khorshidi Paji, Z., Eslamifar, M., "A novel biological synthesis of gold nanoparticle by enterobacteriaceae family", *Tropical Journal of Pharmaceutical Research*, 11 (2012) 887-891.
11. Gholami Shabani, M., Gholami Shabani, Z., Shams Ghahfarokhi, M., Akbarzadeh, A., Riazi, Gh., Razzaghi Abyaneh, M., "Biogenic approach using Sheep milk for the synthesis of Platinum nanoparticles: The role of milk protein in Platinum reduction and stabilization", *International journal of nanoscience and nanotechnology*, 12 (2016) 199-206.
12. Sali Syed, M., Habib Ali Bokhari S., "Gold nanoparticle-based microbial detection and identification", *J. Biomed. Nanotech*, 7 (2011) 229-237.
13. Nam J., Won N., Jin H., Chung H., Kim S., "PH-induced aggregation of gold nanoparticles for photothermal cancer therapy", *J. Am. Chem. Soc*, 131 (2009) 13639-13645.
14. Rai, M., Yadav, A., Cade, A., "Current Trends in Phytosynthesis of Metal Nanoparticles", *Critical Reviews in Biotechnology*, 28 (2008) 277-284.
15. Kumar, V., Yadav, S. C., Yadav, S. K., "Syzygiumc- mini leaf and seed extract mediated biosynthesis of silver nanoparticles and their characterization", *Journal of Chemical Technology & Biotechnology*, 85 (2010) 1301-1309
16. Zhan, G., Huang, J., Du, M., Abdul-Rauf, I., Ma, Y., Li, Q., "Green synthesis of Au-Pd bimetallic nanoparticles: single-step bioreduction method with plant extract", *Materials Letters*, 65 (2011) 2989- 2991.
17. Nadagouda, M. N., Varma, R. S., "Green synthesis of silver and palladium nanoparticles at room temperature using coffee and tea extract", *Green Chemistry*, 10 (2008) 859-862.
18. Philip, D., "Green synthesis of gold and silver nanoparticles using hibiscus rosa sinensis", *Physica E*. 42 (2010) 1417-1424.
19. Das, R. K., Borthakur, B. B., Bora, U., "Green synthesis of gold nanoparticles using ethanolic leaf extract of centella asiatica", *Materials Letters*, 64 (2010) 1445-1447.
20. Kaviya, S., Santhanalakshmi, J., Viswanathan, B., Muthumary, J., Srinivasan, K., "Biosynthesis of silver nanoparticles using citrus sinensis peel extract and its antibacterial activity," *Spectrochimica Acta Part A: Molecular and Biomolecular Spectroscopy*, 79 (2011) 594-598.
21. Song, J. Y., Kim, B. S., "Biological synthesis of bimetallic Au/Ag nanoparticles using persimmon (*Diopyros kaki*) leaf extract", *Korean Journal of Chemical Engineering*, 25 (2008) 808-811.

22. Song, J. Y., Kwon, E. Y., Kim, B. S., "Biological synthesis of platinum nanoparticles using diopyros kaki leaf extract", *Bioprocess and Biosystems Engineering*, 33 (2010) 159-164.
23. Shakeel, A., Saifullah, M. A., Babu Lal, S., Saiqa, I., "Green synthesis of silver nanoparticles using *Azadirachta indica* aqueous leaf extract", *Journal of Radiation Research and Applied Sciences*, 9 (2016) 1-7.
24. Varaprasad, T., Govindh, B., Venkateswara, B., "Green Synthesized Cobalt Nanoparticles using *Asparagus racemosus* root Extract & Evaluation of Antibacterial activity", *Int. J. Chem. Tech. Research*, 10 (2017) 339-345.
25. Hoti, M. S. L., Mehlhorn, H., Barnard, D. R., Benelli, G., "Novel synthesis of silver nanoparticles using *Bauhinia variegata*: a recent ecofriendly approach for mosquito control", *Parasitol Res.*, 115 (2016) 723-733.
26. Vibhute, S. K., Kasture, V. S., Kendre, P. N., Wagh, G. S., "Synthesis of silver nanoparticles from *Moringa Oleifera* : formulation and evaluation against *Saintcaldia albicans*", *Indo American Journal of Pharmaceutical Research*, 4 (2014) 1581-1587.
27. Rout, Y., Behera, S., Ojha, A. K., Nayak, P. L., "Green synthesis of silver nanoparticles using *Ocimum sanctum* (Tulashi) and study of their antibacterial and antifungal activities", *Journal of Microbiology and Antimicrobials*, 4 (2012) 103-109.
28. Sundararajan, B., Ranjitha Kumari, B. D., "Biosynthesis of silver nanoparticles in *Lagerstroemia Speciosa* pers and their antimicrobial activities", *International journal of pharmacy and pharmaceutical sciences*, 6 (2014) 30-34.
29. Sondi, I., Salopek-sondi, B., "Silver nanoparticles as antimicrobial agent: a case study on *E. Colias* a model for gram negative bacteria", *J-colloid interface sci*, 275 (2004) 177-182.
30. Palaniyandi, V., Jayabrata, D., Raman, P., Baskaralingam, V., Kannaiyan, P., "Greener approach for synthesis of antibacterial silver nanoparticles using aqueous solution of neem gum (*Azadirachta indica*L.)", *Industrial crops and products*, 66 (2015) 103-109.